

RESEARCH ARTICLE

The *Drosophila melanogaster* attP40 docking site and derivatives are insertion mutations of *msp-300*

Kevin van der Graaf ^{*}, Saurabh Srivastav, Pratibha Singh, James A. McNew, Michael Stern

Department of Biosciences, Program in Biochemistry and Cell Biology, Rice University, Houston, Texas, United States of America

* kv19@rice.edu



OPEN ACCESS

Citation: van der Graaf K, Srivastav S, Singh P, McNew JA, Stern M (2022) The *Drosophila melanogaster* attP40 docking site and derivatives are insertion mutations of *msp-300*. PLoS ONE 17(12): e0278598. <https://doi.org/10.1371/journal.pone.0278598>

Editor: Efthimios M. C. Skoulakis, Biomedical Sciences Research Center Alexander Fleming, GREECE

Received: September 30, 2022

Accepted: November 19, 2022

Published: December 14, 2022

Copyright: © 2022 van der Graaf et al. This is an open access article distributed under the terms of the [Creative Commons Attribution License](https://creativecommons.org/licenses/by/4.0/), which permits unrestricted use, distribution, and reproduction in any medium, provided the original author and source are credited.

Data Availability Statement: All relevant data are within the paper. Fly stocks are available upon request by contacting researchdata@rice.edu.

Funding: The study was funded by the National Institute of Neurological Disorders and Stroke (grants R01 NS102676 and R21 NS111340) to both MS and JAM. The funders had no role in study design, data collection and analysis, decision to publish, or preparation of the manuscript.

Abstract

The ϕ C31 integrase system is widely used in *Drosophila melanogaster* to allow transgene targeting to specific loci. Over the years, flies bearing any of more than 100 attP docking sites have been constructed. One popular docking site, termed attP40, is located close to the *Nesprin-1* orthologue *msp-300* and lies upstream of certain *msp-300* isoforms and within the first intron of others. Here we show that attP40 causes larval muscle nuclear clustering, which is a phenotype also conferred by *msp-300* mutations. We also show that flies bearing insertions within attP40 can exhibit decreased *msp-300* transcript levels in third instar larvae. Finally, chromosomes carrying certain “transgenic RNAi project” (TRiP) insertions into attP40 can confer pupal or adult inviability or infertility, or dominant nuclear clustering effects in certain genetic backgrounds. These phenotypes do not require transcription from the insertions within attP40. These results demonstrate that attP40 and insertion derivatives act as *msp-300* insertional mutations. These findings should be considered when interpreting data from attP40-bearing flies.

Introduction

For several years, *Drosophila melanogaster* investigators have used a genome integration method based on the site-specific ϕ C31 integrase [1] to target transgenes to specific loci [2]. With this method, ϕ C31 integrase catalyzes sequence-directed recombination between a phage attachment site (attP, present within each of >100 attP “docking sites” in *Drosophila melanogaster*) and a bacterial attachment site (attB, present within the integrating plasmid) [3–7]. By allowing transgene insertion into specific, defined, docking site sequences, the ϕ C31 integrase method increases the reproducibility and decreases the variability of transgene expression observed with the random transgene integration utilized by P elements.

Two docking sites, attP2, located at position 68A4 on chromosome III and attP40, located at position 25C on chromosome II, are widely used docking sites for LexA drivers and Gal4--driven Transgenic RNAi Project (TRiP) insertions [8]. These two attP docking sites are favorable because they express inserted transgenes at high levels while maintaining low basal

Competing interests: The authors have declared that no competing interests exist.

expression [9]. In fact, the *Drosophila melanogaster* stock center at Bloomington, IN, reports possessing 16,503 *Drosophila melanogaster* lines carrying *attP40* and 14,970 lines carrying *attP2*; most lines carry TRiP insertions or the activation domains or DNA binding domains from the Janelia split-Gal4 collection (Annette Parks, personal communication). Although originally reported to be located in an intergenic region, between *CG14035* and *msp-300* [10], *attP40* lies within the first intron of certain *msp-300* isoforms ([11] FlyBase FB2022_02). This observation raises the possibility that *attP40* might act as an insertional mutation for *msp-300*. Indeed, it was previously reported that certain insertions into *attP40* could cause spreading of the H3K27me3 mark over the large *msp-300* exon [12]. Thus, transgenes inserted within the *attP40* docking site might affect expression of at least a subset of *msp-300* isoforms.

MSP-300 (Muscle-specific protein 300 kDa) is a nuclear-associated Nesprin1 orthologue and a component of the Linker of Nucleoskeleton and Cytoskeleton (LINC) complex [13, 14]. The C-terminal domain contains a Klarsicht/Anc1/Syne Homology (KASH) domain that interacts with Sad1p/UNC-84 (SUN)- domain-containing proteins, connecting the outer and inner nuclear membranes [15, 16]. In *Drosophila melanogaster* larvae, *msp-300* transcription has been reported in muscle (Volk, 1992) and fat body [17]. In larval muscle, *msp-300* forms striated F-actin-based filaments that lie between muscle nuclei and postsynaptic sites at the neuromuscular junction. MSP-300 also wraps around immature boutons in response to electrical activity and is required for postsynaptic RNA localization and synaptic maturation [18]. MSP-300 is also required for normal nuclear localization in muscle cells and for integrity of muscle cell insertion sites into the cuticle [14, 19, 20]. MSP-300 isoforms lacking the KASH domain confer deficits in larval locomotion, localization of the excitatory neurotransmitter receptor GluRIIA at the neuromuscular junction (NMJ), and proper NMJ functioning, independently of its role in muscle nuclear positioning [21]. Non-muscle deficits conferred by *msp-300* mutations include defects in oocyte development and female fertility [22]. In humans, mutations in the Nesprin family are associated with several musculoskeletal disorders, including bipolar disorder, autosomal recessive cerebellar ataxia type 1 (ARCA1), X-linked Emery-Dreifuss muscular dystrophy (EDMD) and are risk factors for schizophrenia and autism [23].

Here, we show that flies carrying *attP40* exhibits a nuclear clustering phenotype in larval muscle, which suggests that *attP40* is an *msp-300* insertional mutation. Further, we show that inserting transgenes into *attP40* can increase severity of this phenotype. We use quantitative RT-PCR (Q-PCR) to show that insertions within *attP40* decrease *msp-300* transcript levels in 3rd instar larvae. Finally, we show that chromosomes carrying certain TRiP insertions constructed from the *Valium 20* vector [9] into *attP40* confer recessive lethality or sterility. Because of the variable effects of different transgene insertions into *attP40*, investigators should use caution in interpreting data collected from *Drosophila melanogaster* carrying these insertions.

Materials and methods

Drosophila melanogaster stocks

All fly stocks were maintained on standard cornmeal/agar *Drosophila melanogaster* media: 69.1 g/l corn syrup, 9.6 g/l soy flour, 16.7 g/l yeast, 5.6 g/l agar, 70.4 g/l cornmeal, 4.6 ml/l propionic acid and 3.3 gm/l nipagin. Flies carrying *attP2* and *attP40* lacking insertions were retrieved as white-eyed progeny from transgene insertions carried out at GenetiVision (Houston, TX). The *Drosophila* Stock Center at Bloomington, Indiana provided TRiP *JNK* (#57035), TRiP *spatacsin* (*spat*) (#64868), TRiP *Rop* (#51925), TRiP *Spartin* (#37499), TRiP *atlastin* (*atl*) (#36736), TRiP *Mcu* (#42580), *13XLexAop2-IVS-myr::GFP* (#32210), *LexA::Mef2* (#61543), *CyO-TbA* (#36335), *LexA::nSyb* (#52817), *nSyb-Gal4* (#51635) UAS-*atl*RNAi [24, 25]. All

experiments were performed on *Drosophila melanogaster* that had been reared and maintained at room temperature (22°C) with a 12h:12h light:dark cycle unless otherwise indicated.

Immunocytochemistry

All larvae were dissected in HL3.1 [26] in a magnetic chamber, and fixed in 4% paraformaldehyde for 10 minutes, then washed in PBS with 0.3% Triton-X (PBS-T) and blocked for 30 minutes in PBS-T with 1% BSA. Samples were incubated overnight at 4°C with primary antibody, washed thoroughly with PBS-T and then incubated for 2.5 hours at room temperature with secondary antibody. Samples were then washed with PBS-T and mounted in VectaShield Anti-fade Mounting Medium containing DAPI (Vector laboratories; H-1200-10).

Alexa Fluor® 647 phalloidin (1:200) was used to visualize F-actin. All images were acquired on a Zeiss LSM800 with an Airyscan confocal microscope.

Nuclear clustering analysis

Third instar larval body wall muscle 6 was chosen for all nuclear clustering analysis. Images were opened in ImageJ and nuclei clusters in muscle 6 were counted. We defined a “cluster” as two or more nuclei in which the distance between two nuclear borders was less than five microns. We analyzed six larvae from hemisegments A2-A4 (18 hemisegments total) for each genotype.

Microsoft excel was used to import all nuclear clustering data. “Normal” muscles contained no clusters. For muscles that contained cluster(s), we determined cluster number and nuclei number per cluster. Cluster sizes for each genotype were plotted on a frequency histogram. The percentage of normal hemisegments for each genotype was plotted on a column graph. For each hemisegment we calculated the percentage of nuclei in clusters using the following calculation: number of nuclei within clusters divided by total number of nuclei in muscle 6 multiplied by 100. Then, the average of three hemisegments per larva was calculated and plotted on a column graph. Data was visualized and analyzed using GraphPad Prism v9.3.1 or Synergy Software KaleidaGraph v4.5.2.

Quantitative RT-PCR (Q-PCR)

Primers were designed with PrimerBLAST software according to the published sequence of *msp-300*. We amplified and analyzed two *msp-300* regions: first, the 3' end region, which amplifies transcripts *RD*, *RG*, *RH*, *RI*, *RJ*, *RK*, *RL* and *RM* (transcripts that contain the KASH domain), and second, the middle region, which amplifies transcripts *RB* and *RF* (*B/F*) (transcripts that lack the KASH domain) (Fig 1). For the 3' end region, we used the forward primer sequence 5' -TCAACCTCTTCCAATGCAGGC-3', and the reverse primer sequence 5' -CGC CAGAACCGTGGTATTGA-3'. The *B/F* forward primer sequence was 5' -CACGTACTTGCC GCACGAT-3', and *B/F* reverse primer sequence was 5' -ATTTTTGACACGTTCCCGGC-3'. For amplification of *Rp49*, chosen as the housekeeping gene, the forward primer sequence was 5' -TGTCCCTCCAGCTTCAAGATGACCATC-3' and the reverse primer sequence was 5' -CTTGGGCTTGCGCCATTTGTG-3'. Total RNA (500 ng) was extracted from frozen whole larvae and larval fillets with Direct-zol™ RNA MicroPrep (Zymo Research) according to manufacturer's protocol. The yield of RNA was estimated with the Nanodrop2000 (ThermoFisher). The A₂₆₀:A₂₈₀ ratio was between 1.8–2.1. Superscript™ III First-Strand Synthesis System (ThermoFisher) was used to generate cDNA according to manufacturer's protocol. Reverse transcribed cDNA was then amplified in a 20 µl PCR reaction by the ABI Prism 7000 system (Applied Biosystems) with the universal conditions: 50°C for 2 min, 95°C for 10 min, and 40 cycles (15s at 95°C, 1 min at 60°C). Each sample contained 10 whole larvae. Three separate

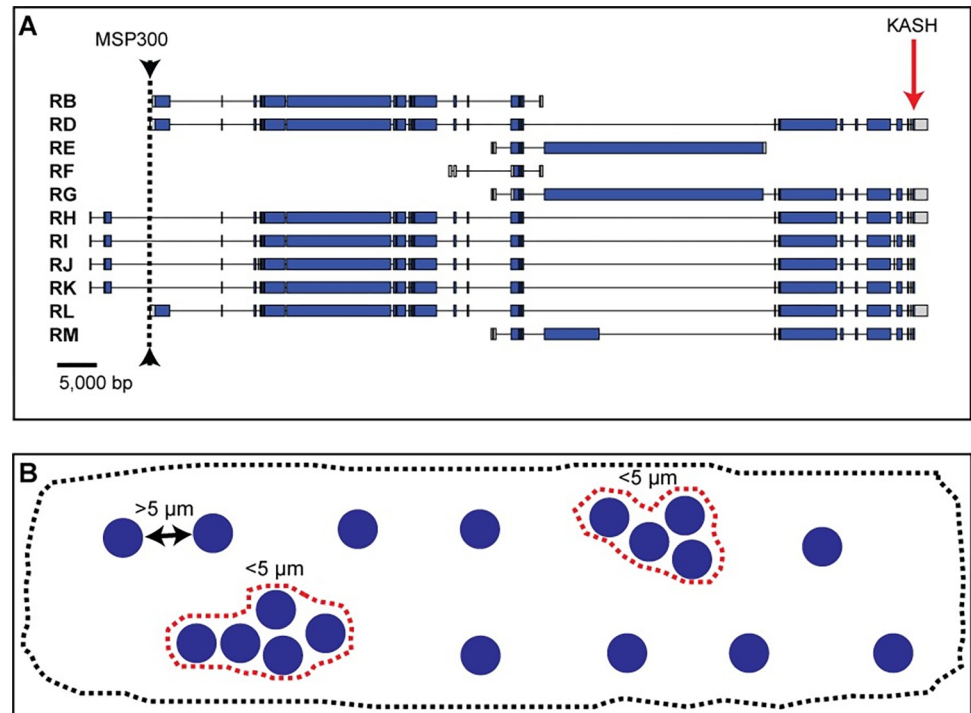


Fig 1. Overview of *msp-300* transcripts and nuclear clustering measurements. A) Overview of the 11 annotated *msp-300* transcripts in *Drosophila melanogaster*. Arrowhead/dotted line indicates location of the *attP40* docking site. Predicted exons shown with blue bars (translated regions) or gray bars (5' UTR or 3' UTR), introns with thin lines. Location of the KASH domain is indicated by red arrow. B) Schematic representation of nuclear clustering in larval body wall muscle 6. If borders between two nuclei are less than 5 μm apart it is counted as a cluster (dotted red lines). Dotted gray line outlines muscle 6.

<https://doi.org/10.1371/journal.pone.0278598.g001>

biological samples were collected from each genotype, and triplicate measures of each sample were conducted for amplification consistency. Data were analyzed with the relative $2^{-\Delta\Delta\text{Ct}}$ method to ensure consistency [27].

Pupal size measurements

We measured length and width in pupae homozygous for each of six TRiP lines and the *attP40* parent chromosome. Pupal length was determined from top to bottom, excluding the anterior and posterior spiracles. Pupal width was determined by measurement at the midpoint along the pupal anterior/posterior axis.

Viability measurements

Each of six TRiP lines were placed in combination with balancer “*CyO-TbA*” [28], which carries the *Tb¹* dominant “Tubby” marker and enabled us to unambiguously genotype balancer-containing from balancer-lacking larvae, pupae and adults. Each of these six TRiP lines were then brother-sister mated and F1 progeny reared in uncrowded vials. The number of Tubby and non-Tubby pupae were counted. Non-Tubby pupae were removed and placed into fresh vials. After seven days, the number of successful eclosions was counted. To monitor viability in the control *attP40* line, pupae reared in uncrowded vials were collected and after seven days the number of successful eclosions was counted.

Fertility measurements

We measured male and female fertility in adults homozygous for each of six TRiP lines and the *attP40* parent chromosome. To measure male fertility, single males were placed in vials with two phenotypically wildtype and fertile virgin females, and ability to generate larval progeny was measured. To measure female fertility, single females were placed in vials with two phenotypically wildtype and fertile males, and ability to generate larval progeny was measured.

Construction of Aop-*atl*RNAi

We chemically synthesized the reported sequence of the TRiP *atl* short hairpin with *Xho*I and *Xba*I sites added to the left and right ends, respectively. (TCGAGAGTCTGGTATAGGTCATTAGTTTAtagttatattcaagcataTAAACTAATGACCTATACCAGGCT—lower case letters indicate the loop sequence). This construct was introduced into the *Xho*I-*Xba*I sites of *pJFRC19-13XlexAop2* (Addgene, Inc) and introduced into embryos at the *attP40* site using with ϕ C31-mediated recombination (GenetiVision, Houston TX). Insert-containing flies were recognized by eye color.

Statistical analysis

For percentage of nuclei in clusters analysis, a One-way ANOVA with Tukey post hoc test was performed. For pupa length and width analysis, a One-way ANOVA with Bonferroni post hoc test was performed. All statistical tests were performed in GraphPad Prism v9.3.1.

Results

The *attP40* docking site is located within or upstream of *msp-300*, depending on the isoform

attP2 and *attP40* are two widely used *attP* docking sites in *Drosophila melanogaster* for insertions of LexA drivers, Gal4-driven TRiP insertions, and other constructs. Both docking sites provide high levels of induced transgene expression while maintaining low basal expression. As of February 2022, the Bloomington *Drosophila* Stock Center (Bloomington, IN) provides 16,503 stocks carrying *attP40* and 14,941 stocks carrying *attP2* (Annette Parks, personal communication). The *attP40* chromosomal location is closest to *msp-300*, which expresses 11 different isoforms. *attP40* lies within intron 1 for transcripts RH, RI, RJ and RK and upstream of transcripts RB, RD, RE, RF, RG, RL and RM (Fig 1A). These results raise the possibility that *attP40* could affect *msp-300* transcript levels. Indeed, De et al. [12] reported that certain transgene insertions into *attP40* alter the H3K27me3 epigenetic mark over at least a part of *msp-300*. Similarly, in a Ph.D. thesis, Cypranowska showed that *attP40* decreased *msp-300* transcription in certain genetic backgrounds and conferred synaptic phenotypes at the larval neuromuscular junction consistent with decreased *msp-300* activity [29].

Given previous reports that *msp-300* variants alter muscle myonuclear spacing [14, 30], we hypothesized that effects of *attP40* on *msp-300* expression might alter larval muscle nuclear clustering. To address this hypothesis, we first defined a “cluster” as two or more nuclei in which the distance between two nuclear borders was less than 5 μ m (Fig 1B). Then, for every nucleus in a larval body wall muscle, we measured the distance to its nearest neighbor, using larval body wall muscle 6 as assay platform. Using this approach, we observed abnormalities in nuclear positioning in larvae homozygous for *attP40* vs. control larvae (homozygous for *attP2*) or larvae heterozygous for *attP40* and *attP2* (Fig 2A–2C). In particular, larvae homozygous for *attP40* (Fig 2D, middle panel) exhibited more nuclear clusters and clusters of greater size than control (Fig 2D, top panel) or heterozygous larvae (Fig 2D, bottom panel), and a significantly

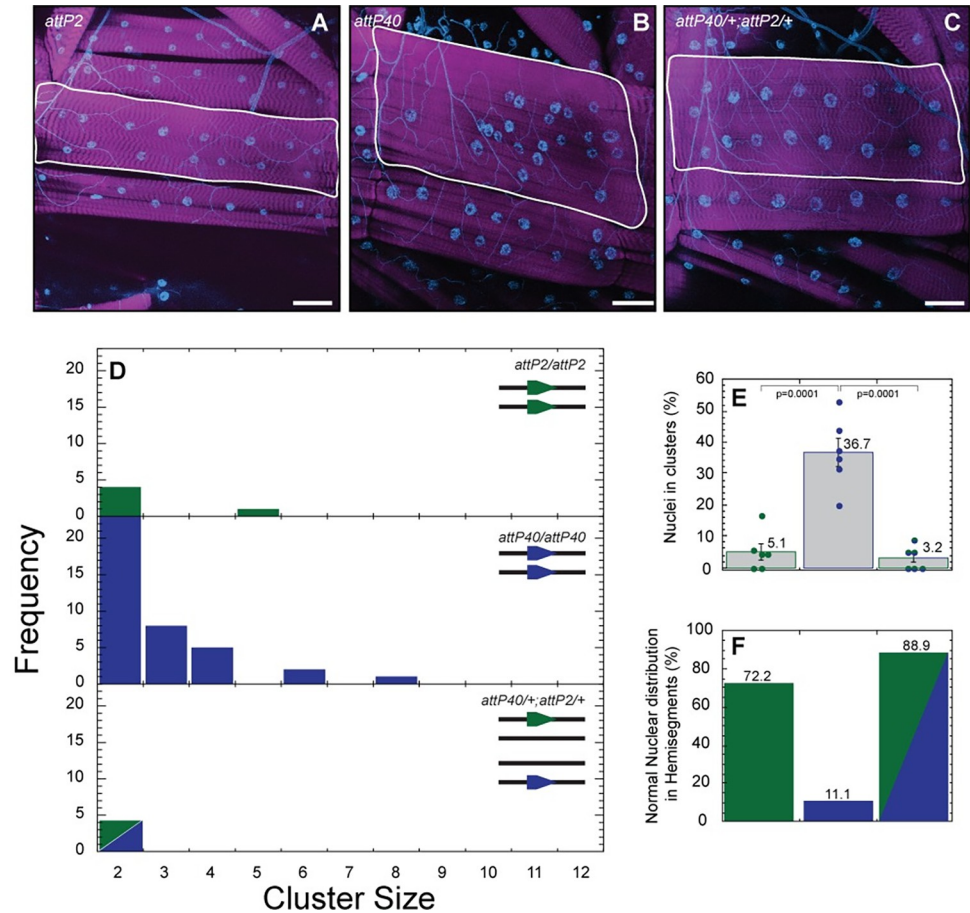


Fig 2. Muscle nuclei clustering phenotype observed in *attP40* larvae. A–C) Representative images of nuclei positioning within muscle 6 for larvae carrying *attP2* (A), *attP40* (B) and *attP40/+; attP2/+* (C). Nuclei are labeled with DAPI (blue), and muscle actin is labeled with phalloidin (magenta). Muscles are outlined with white lines. D) Frequency distribution of the number of nuclei within each cluster within muscle 6 for each genotype shown in upper right. Lines in upper right depict the genotype of each homologue; green pentagons indicate the *attP2* docking site, blue pentagon depicts *attP40* docking site E) Percentage of nuclei found within clusters for each genotype. Means \pm SEMs are shown. The following calculation was used: ((number of nuclei within clusters / total number of nuclei) \times 100). F) Percentage of hemisegments with normal nuclear distribution within muscle 6. *attP2* is represented in green, *attP40* in blue and *attP40/+; attP2/+* in half green/half blue for panels D–F. For each genotype 3 hemisegments per larvae for 6 larvae total were analyzed. One way ANOVA with Tukey post-hoc test was used for statistical analyses. Scale bar = 50 μ m.

<https://doi.org/10.1371/journal.pone.0278598.g002>

greater number of nuclei within clusters (Fig 2E). As a result, larvae homozygous for *attP40* exhibited fewer hemisegments with a normal nuclear distribution than control or heterozygous larvae (Fig 2F). We conclude that *attP40* causes a recessive muscle nuclear clustering phenotype.

Effects of inserting transgenes into *attP40* on phenotypic severity

To determine if insertions into *attP40* could affect nuclear clustering, we used the functionally neutral *LexAop2-IVS-myr::GFP* reporter introduced into *attP40* and crossed these flies with *attP2*, *attP40*, *lexA::Mef2* or *lexA::nSyb*. Representative images of nuclei clustering in body wall muscle 6 for each genotype is shown in Fig 3A–3D. First, we found that *LexAop2-IVS-myr::GFP/+* larvae (only one copy of *attP40*) showed only 6.18% of nuclei in clusters and a mostly normal nuclear distribution (Fig 3E top panel, 3F and 3G), indicating that *LexAop2-IVS-myr::*

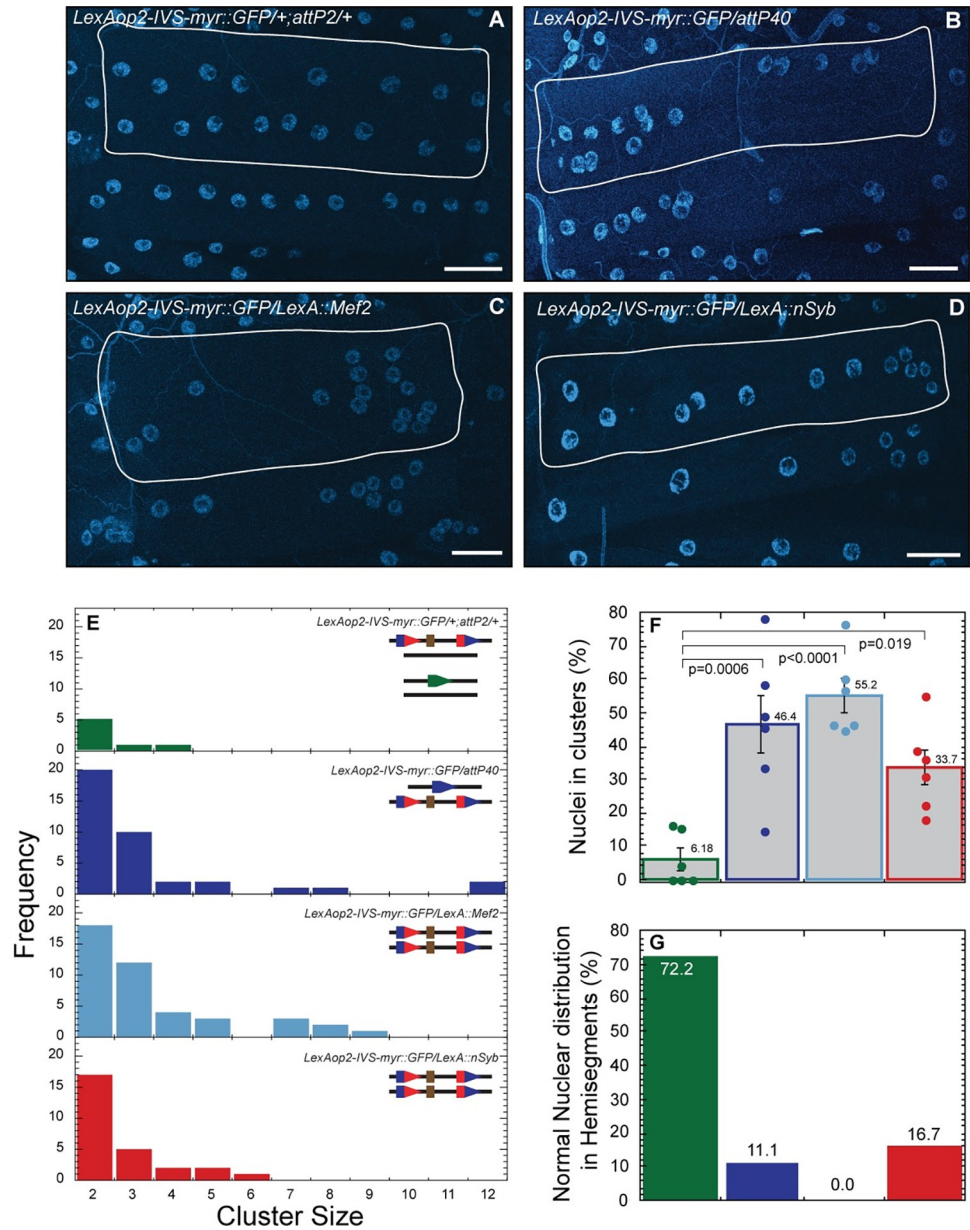


Fig 3. Effects of inserting AOP/LexA transgenes into attP40 on nuclear clustering severity. A-D) Representative images of nuclei position within muscle 6 for *LexAop2-IVS-myr::GFP* in combination with *attP2* (A), *attP40* (B), *LexA::Mef2* (C) and *LexA::nSyb* (D). Nuclei are labeled with DAPI (blue). Muscles are outlined with solid white lines. E) Frequency distribution of the number of nuclei within each cluster within muscle 6 for each genotype indicated in upper right. Lines in upper right show genotype of each chromosome II homologue (in top right histogram, both chromosome II and chromosome III are shown). Green pentagon represents *attP2*, blue pentagons represent *attP40*, red/blue composite pentagons represent *attP40* carrying indicated insertion. Brown rectangle represents insertion. F) Percentage of nuclei found within clusters for each genotype. Means +/- SEMs are shown. The following calculation was used: ((number of nuclei within clusters / total number of nuclei) x 100). G) Percentage of hemisegments with normal nuclear distribution within muscle 6. In panels E-G, each genotype is represented with a different color as follows: *LexAop2-IVS-myr::GFP/attP2* (green), *LexAop2-IVS-myr::GFP/attP40* (blue), *LexAop2-IVS-myr::GFP/LexA::Mef2* (light blue) and *LexAop2-IVS-myr::GFP/LexA::nSyb* (red). For each genotype 3 hemisegments per larvae for 6 larvae total were analyzed. One way ANOVA with Tukey post-hoc test was used for statistical analyses. Scale bar = 50 μ m.

<https://doi.org/10.1371/journal.pone.0278598.g003>

GFP, like “empty” *attP40* (*attP40* lacking an insertion), is recessive. However, when *LexAop2-IVS-myr::GFP* was in combination with empty *attP40*, we found extremely large nuclear clusters (containing up to 12 nuclei; Fig 3E, lower panel in blue), which were not observed in larvae homozygous for *attP40* (Fig 2D). In addition, 46.4% of nuclei were in clusters compared to 36.7% in larvae homozygous for *attP40* (Figs 3F and 2E). Thus, transgene insertion into one *attP40* site increases nuclear clustering severity. To determine if inserting transgenes into both *attP40* sites would affect nuclear clustering, we examined nuclear clustering in *LexAop2-IVS-myr::GFP/LexA::nSyb* larvae and found nuclear clustering similar to larvae homozygous for empty *attP40* (Figs 3E bottom panel and 2D). These results suggest that inserting transgenes into a second *attP40* site has little additional effect on nuclear clustering.

In the experiments described above, the insertions in *attP40* were not transcribed in muscle. Given the previous report [12] that certain transgene insertions into *attP40* could generate epigenetic marks that spread into *msp-300*, potentially altering *msp-300* expression, we determined if expressing the insertions in muscle would affect nuclear clustering. Thus, we created *LexAop2-IVS-myr::GFP/LexA::Mef2* larvae, in which the insertions in each *attP40* site would be expressed in muscle. We found that these larvae exhibited a more severe nuclear clustering phenotype even than *LexAop2-IVS-myr::GFP/empty attP40* (Fig 3E lower panel in cyan, 3F and 3G), and was the only genotype tested in which every muscle exhibited some nuclear clustering (Fig 3G). These observations suggest that transcribing insertions in *attP40* might further increase the severity of nuclear clustering phenotype.

To determine if Gal4-regulated insertions, like LexA-regulated insertions, would also induce nuclear clustering, we investigated properties of one Gal4-driven shRNA construct (targeting *spatacsin* (*spat*) (CG13531)), created by the transgenic RNAi project (TRiP) [9], as our example. We chose a TRiP insertion for this study because these insertions are widely used in the community and TRiP insertions represent more than half (8,884) of *attP40* insertions maintained at the Drosophila stock center in Bloomington, IN. Representative images are shown in Fig 4A–4C. We found that TRiP *spat/+;attP2/+* larvae exhibited wildtype nuclear positioning (Fig 4D, top panel, 4E and 4F), but both TRiP *spat/empty attP40* or homozygous TRiP *spat* exhibited a strong nuclear clustering phenotype (Fig 4D middle and bottom panel, 4E and 4F)—in fact, larvae homozygous for TRiP *spat* exhibited clusters up to 15 nuclei in size (Fig 4D). Thus, TRiP *spat* confers a recessive clustering phenotype, which indicates that this Gal4-driven transgene insertion behaves in a manner similar to the LexA insertions described above.

Effects of attP40 and derivatives on msp-300 transcript levels

We hypothesized that nuclei clustering in larvae homozygous for *attP40* and derivatives reflected altered expression of at least some of the eleven *msp-300* isoforms (Fig 1). To test this hypothesis, we prepared RNA from whole third instar larvae and performed quantitative RT-PCR (Q-PCR) using primers from two regions of the *msp-300* transcription unit; first, the far 3' end of *msp-300*, which includes the KASH domain and accounts for eight of eleven annotated transcripts [16], see Fig 5A, and second, an internal region that is predicted to amplify the *RB* and *RF* transcripts, which lack the KASH domain. Thus, these primers enable analysis of 10 of 11 annotated transcripts (Fig 5A).

We found using the 3' end primers that *msp-300* transcript levels were decreased about two-fold in larvae homozygous for *attP40* and that contained an insertion in at least one of the *attP40* sites (Fig 5B). These results support the possibility that *attP40* derivatives cause nuclei clustering by decreasing *msp-300* transcript levels. These effects on transcript levels, like effects on nuclear clustering, were recessive, as *msp-300* transcript levels in *LexAop2-IVS-myr::GFP/+* or TRiP *spat/+* larvae were not distinguishable from those from the *attP2* control.

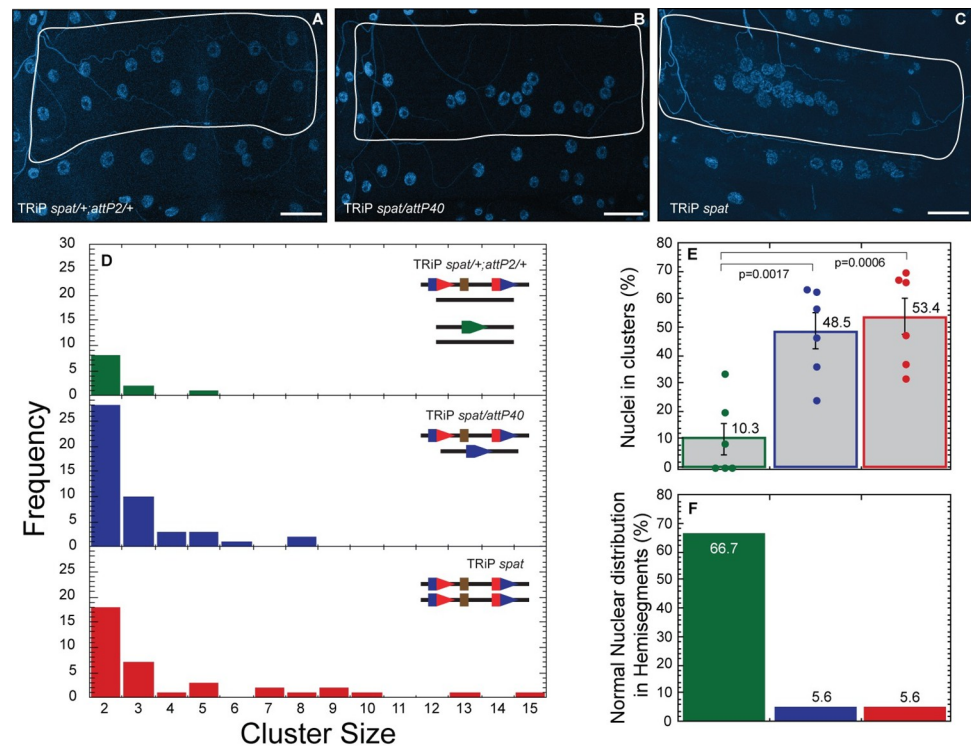


Fig 4. Effects on nuclei clustering of inserting Gal4-regulated TRiP *spatacsin* (*spat*) into *attP40*. A–C) Representative images of nuclear position within muscle 6 for TRiP *spat*^{+/+}, *attP2*^{+/+} (A), TRiP *spat*/*attP40* (B) and TRiP *spat* (C). Nuclei are labeled with DAPI (blue). Muscles are outlined with solid white lines. D) Frequency distribution of the number of nuclei within each cluster within muscle 6 for each genotype indicated in upper right. Lines in upper right show genotype of each chromosome II homologue (in top right histogram, both chromosome II and chromosome III are shown). Green pentagon represents *attP2*, blue pentagons represent *attP40*, red/blue composite pentagons represent *attP40* carrying indicated insertion. Brown rectangle represents insertion. E) Percentage of nuclei found within clusters for each genotype. Means \pm SEMs are shown. The following calculation was used: ((number of nuclei within clusters / total number of nuclei) \times 100). F) Percentage of hemisegments with normal nuclear distribution within muscle 6. Each genotype is represented with a different color in panels D–F with TRiP *spat*^{+/+}, *attP2*^{+/+} (green), TRiP *spat*/*attP40* (blue) and TRiP *spat* (red). For each genotype 3 hemisegments per larvae for 6 larvae total were analyzed. ANOVA with Tukey was used for statistical analyses. Scale bar = 50 μ m.

<https://doi.org/10.1371/journal.pone.0278598.g004>

We were surprised to find that larvae homozygous for empty *attP40* exhibited wildtype *msp-300* transcript levels, despite exhibiting a strong nuclear clustering phenotype. However we note that *msp-300* is transcribed in larval fat bodies as well as muscle [17]; thus our whole larva RNA preparations might not capture *attP40* transcriptional effects specifically in muscle. To address this possibility, we performed Q-PCR on RNA prepared from larval fillets, in which the fat body as well as all other internal organs were removed, leaving only the body wall muscles, underlying epidermis, and cuticle. We found that with this semi-purified muscle tissue as RNA source, empty *attP40* fillets as well as *LexAop2-IVS-myr::GFP/LexA::Mef2* fillets exhibited a \sim two-fold decrease in *msp-300* transcript levels (Fig 5C), similar to what we observed in whole larvae carrying *attP40* insertions (Fig 5B). Thus, muscle *msp-300* transcript levels match muscle *msp-300* phenotypes in *attP40* and derivatives. These results also raise the possibility that empty *attP40* might increase levels of certain *msp-300* isoforms in non-muscle tissues.

The primers used in Fig 5B enable amplification of KASH domain isoforms. To analyze transcript levels of the two annotated non-KASH domain isoforms, transcripts *RB* and *RF*, we used the internal primers described above to amplify RNA from whole larvae. We found that

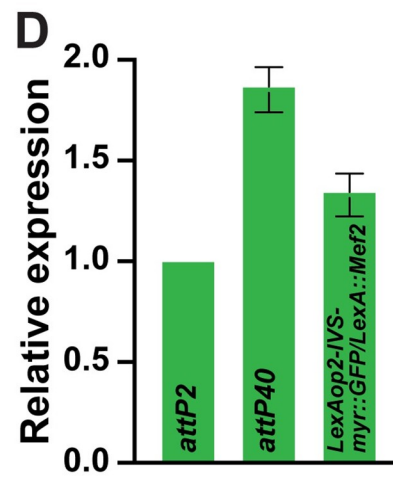
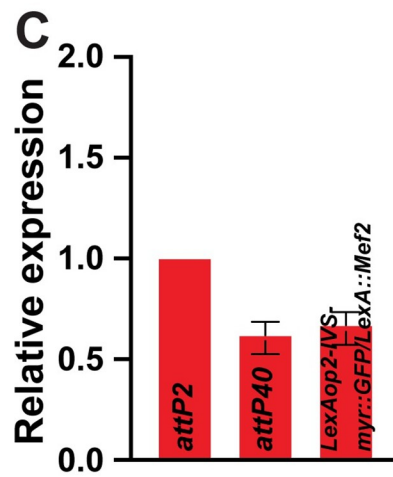
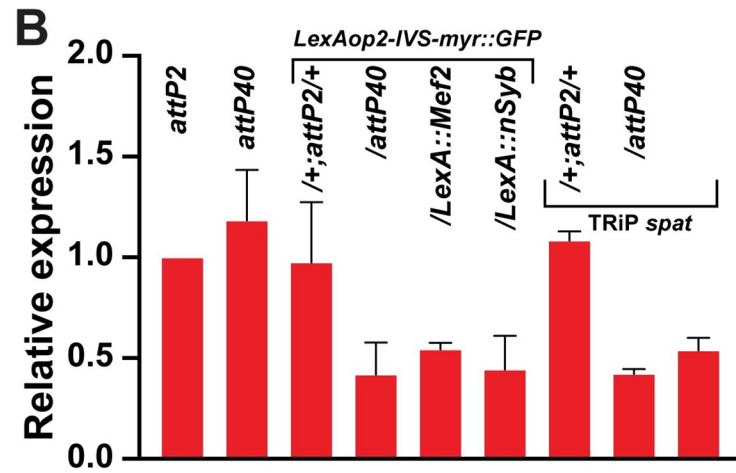
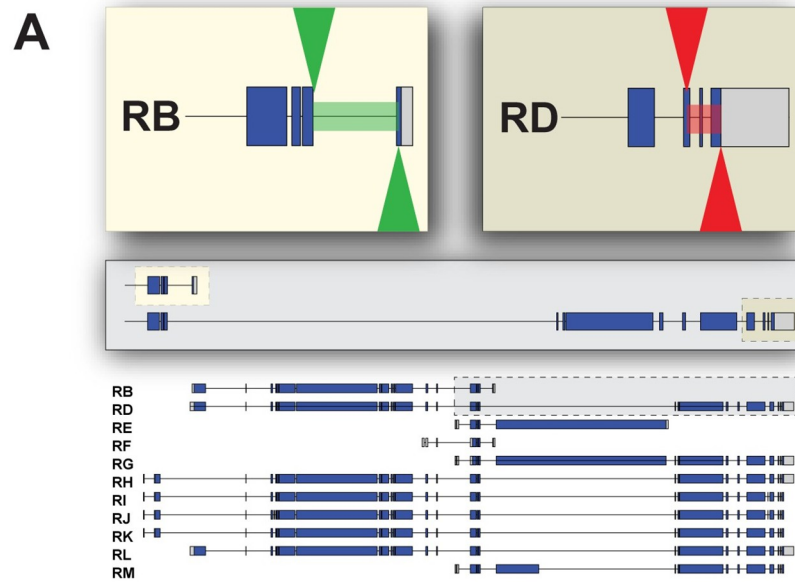


Fig 5. Effect of attP40 and derivatives on msp-300 transcript levels. A) Schematic overview of the primer set used in this analysis (green arrowheads for mid region primers, red arrowheads for 3' primers). Grey inset enhances the mid to 3' end region of transcripts RB and RD. The (light color) inset shows the primer locations used to analyze transcripts RB and RF. The (dark color) inset show the primer locations used to analyze transcripts RD, RG, RH, RI, RJ, RK, RL and RM (KASH-containing transcripts). Annotated transcripts as shown in Fig 1. B) Quantitative RT-PCR (Q-PCR) was used to measure msp-300 KASH-containing transcript levels, normalized to attP2, from whole third instar larvae of the indicated genotypes. C) Q-PCR was used to measure msp-300 KASH-containing transcript levels, normalized to attP2, from 3rd instar larval fillets of the indicated genotypes. D) Q-PCR was used to measure msp-300 transcripts B and F, normalized to attP2, from whole third instar larvae of the indicated genotypes. Red bars represent transcript levels measured with msp-300 KASH-containing primers and green bars represent transcript levels measured with transcripts B and F primers. Mean +/- SEM was determined from at least three separate biological samples collected from each genotype, and triplicate measures of each sample. The 2^{-ΔΔCt} was employed for this measurement. Each sample contained a mix of 10 whole larvae for (B) and (D) or a mix of 5 larval fillets (C).

<https://doi.org/10.1371/journal.pone.0278598.g005>

unlike the case with the KASH domain transcripts, non-KASH domain transcripts were increased in both empty attP40 and *LexAop2-IVS-myr::GFP/LexA::Mef2* larvae (Fig 5D). Phenotypic consequences of these altered transcript levels are not clear. Thus, attP40 can have distinct effects on transcript levels of different isoforms.

Effects of TRiP insertions into attP40 on viability and fertility

Many transgenes introduced into attP40 are RNAi short hairpin sequences from the “TRiP” project cloned into the *Valium20* vector. We noticed some unexpected viability phenotypes, even in the absence of expression, when working with some of these insertions, so we wanted to characterize TRiP insertion viability systematically. However, monitoring TRiP insertions for recessive viability and fertility was problematic for two reasons. First, many TRiP insertions into attP40 are balanced with *CyO*; this is problematic because the *Cy¹* “Curly” dominant marker on the *CyO* balancer is unreliable. The Curly wing phenotype is easily suppressed by genetic modifiers as well as the environmental conditions of low temperature and larval crowding [31]; indeed, the FlyBase allele report for *Cy¹* states that *Cy¹* “frequently overlaps [wildtype] at 19°C. some balanced *Cy* chromosomes pick up suppressors of *Cy* in stock” (<http://flybase.org/reports/FBal0002196.html>). Second, the *y⁺* and *v⁺* markers used for the TRiP insertions are each fully dominant, unlike the semi-dominant mini-white marker used on other transgenes. Because of these two features, it is difficult to accurately distinguish flies carrying *CyO* from flies without *CyO* by simple visual inspection.

To address these difficulties, we placed several TRiP insertions in combination with a modified *CyO* balancer upon which the dominant *Tb¹* “Tubby” transgene had been introduced by P-element mediated transformation [28]. This *CyO-Tb¹* balancer also carries the dominant *Star* marker, which confers “Rough eyes” [32]. Both *Tb¹* and *Star* are completely penetrant.

Table 1. Homozygous viability in TRiP lines.

Genotype	Tubby (T)	Non-Tubby (NT)	NT/Total (%)	Non-Tubby eclosion	Eclosion (%)
<i>attP40</i>	N.A.*	N.A	N.A	87/103	84.5
TRiP <i>JNK/CyO-Tb¹</i>	331	235	41.52%	203/235	86.4
TRiP <i>spat/CyO-Tb¹</i>	285	34	10.66%	0/34	0
TRiP <i>Spartin/CyO-Tb¹</i>	186	106	36.30%	81/106	76.4
TRiP <i>Mcu/CyO-Tb¹</i>	183	83	31.20%	18/83	21.7
TRiP <i>Rop/CyO-Tb¹</i>	353	102	22.42%	27/102	26.5
TRiP <i>atl/CyO-Tb¹</i>	310	0	0.00%	N.A	N.A

*Not Applicable.

<https://doi.org/10.1371/journal.pone.0278598.t001>

Table 2. Adult fertility in TRiP lines.

	Male fertility	Female fertility
<i>attP40</i>	10/10	10/10
TRiP <i>JNK</i>	0/10	10/10
TRiP <i>Spartin</i>	7/10	10/10
TRiP <i>spatacsin</i>	N.A	N.A
TRiP <i>Mcu</i>	2/10	2/10*
TRiP <i>Rop</i>	0/10	2/10**
TRiP <i>atlastin</i>	N.A	N.A

*2 and 11 pupal progenies produced from the two fertile females.

**6 and 11 pupal progenies produced from the two fertile females.

<https://doi.org/10.1371/journal.pone.0278598.t002>

Thus, the use of *CyO-TbA* to balance TRiP insertions enabled us to unambiguously distinguish flies heterozygous from homozygous for each TRiP insertion at the larval, pupal, and adult stages.

From six TRiP insertions tested when homozygous, we found a wide variety of viability and fertility deficits (Tables 1 and 2). The mostly strongly affected insertions, TRiP *atl* and TRiP *spat*, permitted no homozygous viable adults, although a few pupae homozygous for TRiP *spat* were observed. Flies bearing the TRiP *rop* and TRiP *Mcu* insertions were less strongly affected. Pupae homozygous for either insertion were observed, albeit at a lower frequency than expected, and most (~80%) failed to eclose. Escaper adults exhibited greatly decreased fertility (Table 2). In particular, none of the males homozygous for TRiP *rop*, and only 2 of 10 males from TRiP *Mcu*, were fertile. Likewise, most females homozygous for TRiP *rop* and TRiP *Mcu* were infertile, and the rare fertile females produced very few progeny. Flies bearing the TRiP *JNK* insertion were even less strongly affected. Adults homozygous for TRiP *JNK* were plentiful (Table 1), and the females displayed wildtype fertility (Table 2). However, males homozygous for TRiP *JNK* appeared to be completely sterile (Table 2). All phenotypes of flies homozygous for TRiP *spartin* appeared similar to wildtype. TRiP *spartin* was the only one of the six TRiP lines tested for which we were able to construct and maintain a homozygous stock.

Pupae homozygous for TRiP insertions showed body size defects as well as viability or fertility defects. We did not notice any visible defects in the pupa case and posterior/anterior spiracles in four of our TRiP lines (Fig 6A). Pupae homozygous for *spat* usually failed to evert their anterior spiracles (Fig 6B), a phenotype previously observed in mutants defective in ecdysone production [33] or larval muscle function [34]. Although pupal length in these homozygous pupae was not significantly different from the control (pupae homozygous for empty *attP40*), pupal width in these homozygous pupae was significantly decreased (Fig 6C and 6D). The TRiP *Mcu* insertion had the strongest effect on pupal width.

In an attempt to separate the recessive lethality of the TRiP *atl* chromosome from the *attP40* insertion, we performed two rounds of free recombination between TRiP *atl* and another stock with no lethal mutations on chromosome II. However, we were unable to separate the lethality from the TRiP *atl* insertion, indicating that the lethal allele of TRiP *atl* is at or close to the insertion site.

We also tested the viability and fertility of the flies carrying the identical hairpin sequence found in TRiP *atl* but introduced into *attP40* via a different vector. In particular, we introduced the TRiP *atl* hairpin sequence into pJFRC19-13XlexAop2, and then introduced this plasmid into *attP40* with ϕ C31-mediated recombination. We found that flies bearing this *Aop*-

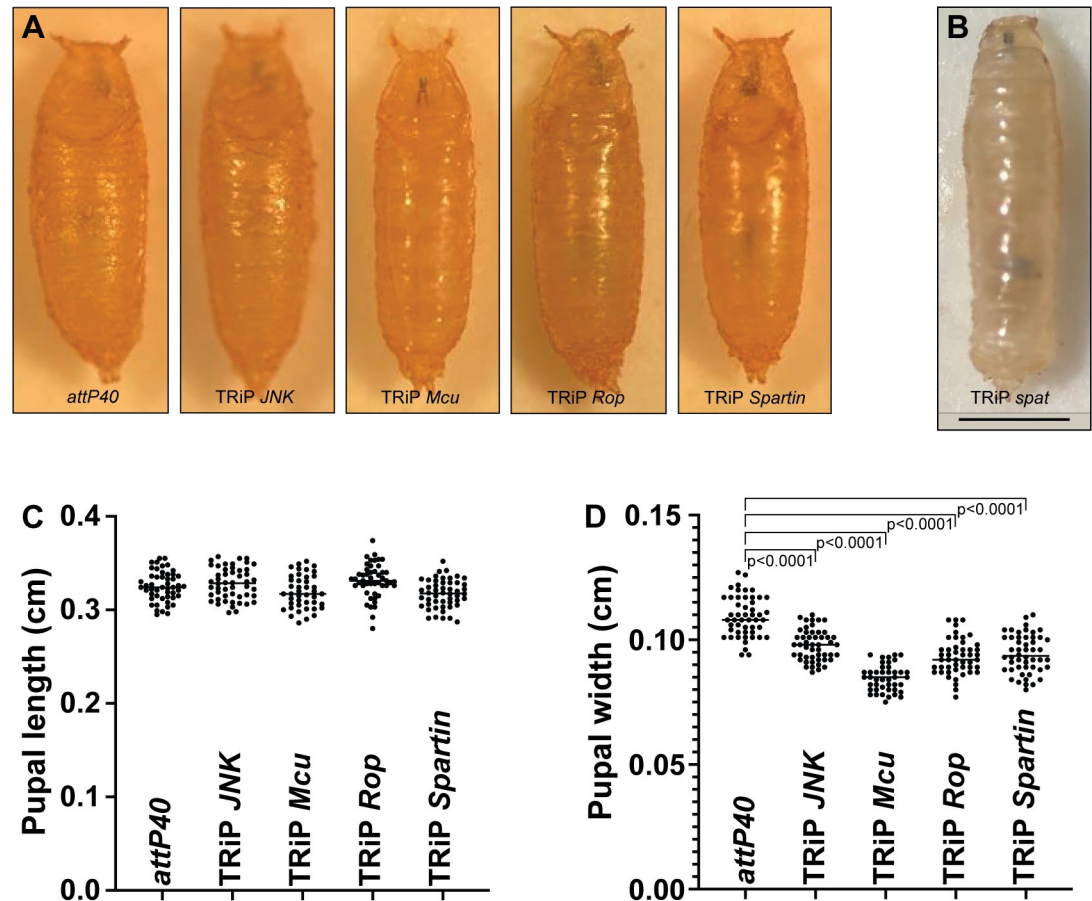


Fig 6. Effects of homozygous TRiP insertions on pupal length and width. A) Visual representation of pupae homozygous for *attP40* and TRiP *JNK*, *Mcu*, *Rop* and *Spartin*. B) Visual representation of an early pupa homozygous for TRiP *spat*. C) Pupal length measurements for the genotypes shown in (A). D) Pupal width measurements for the genotypes shown in (A). For pupa length and width analysis, a One-way ANOVA with Bunnnett post hoc test was performed. Scale bar = 1 mm.

<https://doi.org/10.1371/journal.pone.0278598.g006>

atlRNAi insertion were fully viable and fertile. Therefore, the phenotype conferred by the hair-pin sequence from TRiP *atl* is affected by genetic context.

Dominance and recessiveness of *attP40* and derivatives

Data shown in Figs 2–5 indicate that *attP40* and derivatives are recessive for nuclear clustering and *msp-300* transcription phenotypes. However, in certain genetic backgrounds, we have found that *attP40* and derivatives can have dominant effects on clustering. In particular, we introduced the pan-neuronal *Gal4* driver *nSyb-Gal4* into flies heterozygous for either empty *attP40*, or the TRiP *atl* insertion into *attP40*. Note that *nSyb-Gal4* is not inserted into *attP40* and the stock does not contain *attP40*. We found that the *nSyb-Gal4* background did not have a significant effect on larval muscle nuclear clustering in empty *attP40/+* (Fig 7A, 7D top panel, 7E and 7F); however, TRiP *atl/+* larvae carrying *nSyb-Gal4* displayed nuclear clustering that was significantly increased compared to both empty *attP40/+* and empty *attP40/+; nSyb-Gal4* (Fig 7B, 7D middle panel, 7E and 7F). This phenotype is not a consequence of *atl* knock-down in neurons; when we used *nSyb-Gal4* to drive expression of an *atlRNAi* that was not inserted into *attP40*, we observed no increase in nuclear clustering (Fig 7C, 7D bottom panel, 7E and 7F). Therefore, *attP40* derivatives can confer dominant effects in certain genetic

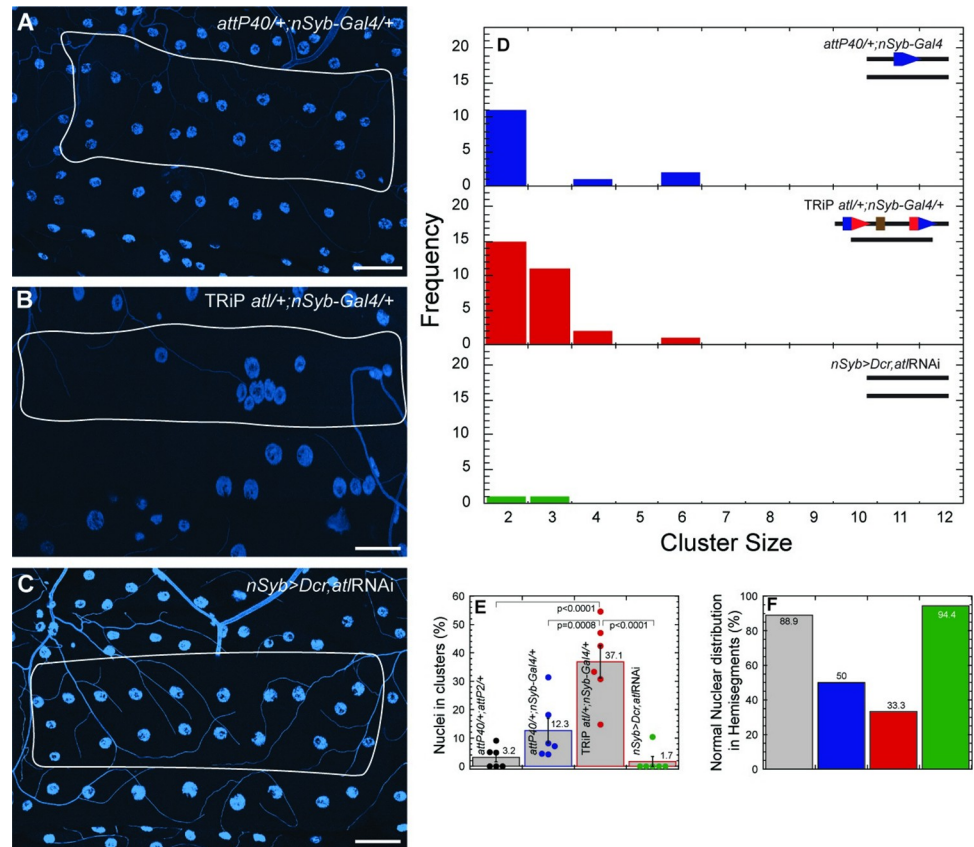


Fig 7. TRiP *atl* can have dominant effects on nuclear clustering in some genetic backgrounds. A-C) Representative images of nuclei position within muscle 6 for *attP40/+; nSyb-Gal4/+* (A), *TRiP atl/+; nSyb-Gal4/+* (B) and *nSyb>Dcr, atlRNAi* (C). Nuclei are labeled with DAPI (blue). Muscles are outlined with solid white lines. D) Frequency distribution of the number of nuclei within each cluster within muscle 6 for each genotype indicated in upper right. Lines in upper right show genotype of each chromosome II homologue. Blue pentagons represent *attP40*, red/blue composite pentagons represent *attP40* carrying indicated insertion. Brown rectangle represents insertion. E) Percentage of nuclei found within clusters for each genotype. Means \pm SEMs are shown. The following calculation was used: ((number of nuclei within clusters / total number of nuclei) \times 100). F) Percentage of hemisegments with normal nuclear distribution within muscle 6. Each genotype is represented with a different color in panels D-F with *attP40/+; attP2/+* (grey), *attP40/+; nSyb-Gal4/+* (blue), *TRiP atl/+; nSyb-Gal4/+* (red) and *nSyb>Dcr, atlRNAi* (green). For each genotype 3 hemisegments per larvae for 6 larvae total were analyzed. ANOVA with Tukey was used for statistical analyses. Scale bar = 50 μ m.

<https://doi.org/10.1371/journal.pone.0278598.g007>

backgrounds. In addition, these results support the conclusion that the TRiP *atl* insertion into *attP40* confers a stronger MSP-300 phenotype than empty *attP40*.

Discussion

Effects of the *attP40* docking site and derivatives on *msp-300*-mediated phenotypes

The *attP40* docking site for *Drosophila melanogaster* transgene integration is widely used for ϕ C31-mediated transgene integration. *attP40* lies within the transcription unit of *msp-300*, which encodes the *Drosophila melanogaster* orthologue of Nesprin-1; this observation raises the possibility that *attP40* is an *msp-300* insertional mutation. Here we show that *attP40*, either alone or containing any of several specific transgene insertions, causes phenotypes similar to *msp-300* mutations, such as larval muscle nuclear clustering and viability deficits. In addition,

attP40-containing larvae exhibit an approximately two-fold decrease in *msp-300* transcript levels of certain isoforms. The effect on nuclear clustering and viability varies depending on the precise transgene introduced into *attP40*. We conclude that *attP40* is an insertional mutation for *msp-300*.

Additional msp-300-dependent and independent phenotypes conferred by attP40

Reports from other investigators are now appearing in which phenotypic consequences of *attP40*-bearing flies are described. In a Ph.D. thesis, Cypranowska (2020) reported that *attP40* decreases *msp-300* transcription and also confers abnormal synapse function at the larval neuromuscular junction [29]. Many of these phenotypes are similar to those conferred by loss of the muscle glutamate receptor *gluRIIA*; this observation is significant because it was previously reported that *gluRIIA* localization is affected by *msp-300* [21]. These observations raise the possibility that *attP40* regulates synaptic transmission via *msp-300*-dependent effects on *gluRIIA*.

Other investigators have reported other *attP40*-dependent phenotypes. For example, Groen *et al.* reported that *attP40* decreases transcription of *ND-13A*, the gene immediately centromere-distal from *attP40* and which encodes a component of mitochondrial complex I [35]. Further, they suggest that this decreased *ND-13A* transcription might mediate the resistance to the chemotherapy agent cisplatin observed in *attP40* flies [35]. More recently, Duan *et al.* reported that *attP40* alters neuronal architecture of the olfactory glomerulus, a phenotype that appears to be *msp-300*-independent [36]. Taken together, these results indicate that *attP40* can confer a variety of phenotypes in a variety of tissues by affecting transcription of at least two genes.

attP40 phenotypes can be dominant or recessive depending on genetic background

We tested if *attP40* and derivatives containing insertions into *attP40* were dominant or recessive for the nuclear clustering and *msp-300* transcription phenotypes. We found that in most cases, the effects of *attP40* and derivatives were recessive. For example, the neutral reporter *LexA-myr-GFP* or the TRiP *spat* insertion within *attP40* each conferred severe nuclear clustering and decreased *msp-300* transcription when homozygous or in combination with empty *attP40*, but not when *attP40* was absent, from the other homologue. These observations indicate that *attP40*-dependent phenotypes are recessive. However, in other genetic backgrounds, we detected dominant effects of *attP40* derivatives. In particular, the TRiP *atl* insertion within *attP40* conferred a dominant nuclear clustering phenotype in a genetic background containing the neuronal Gal4 driver *nSyb-Gal4*. Similarly, Cypranowska reported that *attP40* conferred a dominant 2.7-fold decrease in *msp-300* transcript levels in the presence of the motor neuron Gal4 driver *OK6* [29]. We conclude that the phenotypes of *attP40* and derivatives can be dominant or recessive depending on genetic background.

Effects of specific transgene insertions into attP40 on mutant phenotypes

We tested if the nucleotide sequence of specific transgenes inserted into *attP40* would affect mutant phenotypes. First, we found that transgenes from either the *LexA* or the *Gal4* regulatory systems were capable of enhancing the nuclear positioning phenotype and *msp-300* transcript phenotypes to moderate degrees. Second, we tested if transcription of inserted transgenes in muscle would affect mutant phenotypes. In particular, we compared nuclear

positioning in larvae expressing *LexA-myr-GFP* in neurons vs. muscle and found that muscle expression modestly increased severity of the nuclear clustering phenotype but did not affect *msp-300* transcript levels. These results indicate that muscle transcription of inserted transgenes is not necessary for mutant phenotype, but we are unable to rule out the possibility muscle transcription could contribute to severity of mutant phenotype.

TRiP insertions into attP40: extremely variable degrees of recessive lethality and sterility

Of the 16,503 lines carrying *attP40* maintained at the Drosophila stock center (Bloomington, IN), 8,884 contain TRiP (short hairpin sequences for RNAi) insertions, mostly in the *Valium 20* vector. In studies of six of these lines, we observed a range of recessive phenotypes, from full lethality to full (or partial) sterility to ~wildtype. This extreme variability in phenotypes among the TRiP lines was unexpected, as each line contains inserts with identical sequences, with the exception of the sequence of the short hairpin itself. These results suggest either that phenotypic strength is affected unexpectedly strongly by the precise nucleotide sequence of the hairpin, or alternatively, that these TRiP lines have accumulated genetic modifiers at an unusually high rate, and that these modifiers have variable effects on phenotype. These two possibilities are not mutually exclusive.

Because of the wide variety of phenotypes exhibited by flies carrying distinct TRiP insertions, we wondered if we could predict phenotypes conferred by specific TRiP lines from information presented at the Bloomington Drosophila Stock Center (BDSC, <https://bdsc.indiana.edu>). We noticed that in the description of the six TRiP lines tested, five (TRiP *atl*, TRiP *spat*, TRiP *rop*, TRiP *Mcu*, and TRiP *JNK*) contained the phrase “May be segregating CyO”, or a related phrase. These five lines are the same ones for which we were unable to maintain a homozygous line. The sixth line (TRiP *spartin*), for which we were able to maintain a homozygous line, lacked this phrase. This correspondence raises the possibility that researchers might be able to distinguish homozygous viable and fertile TRiP lines from others by the absence/presence of this phrase. As of the most recent report (from 2019), the BDSC reports that 31.46% of the 8884 TRiP lines in *attP40* (2795 total) are listed as homozygous, with the rest as “CyO”, “CyO fl” or “CyO mix”.

Conclusions

We have shown *attP40* and derivatives containing insertions confer *msp-300* mutant phenotypes and can decrease *msp-300* transcript levels. Regardless of the mechanism underlying the variety of phenotypes conferred by various TRiP insertions within *attP40*, investigators should be aware that these insertions might confer phenotypes that are difficult to predict and might manifest in a variety of ways. Going forward, investigators should use caution when interpreting data resulting from flies containing *attP40*, especially in muscle tissues.

Acknowledgments

The authors would like to thank the Bloomington Stock Center (BDSC) for providing all the fly lines used in this study. We are grateful to Annette Parks (BDSC) for communicating information on BDSC fly stock holdings and to Alekhya Gurram for assistance with Q-PCR experiments. This work was done in part using resources of the Rice University Shared Equipment Authority (<https://research.rice.edu/sea/>). We thank Budi Utama for help with light microscopy and image quantitation.

Author Contributions

Conceptualization: Kevin van der Graaf, James A. McNew, Michael Stern.

Data curation: Kevin van der Graaf.

Formal analysis: Kevin van der Graaf, Saurabh Srivastav, Pratibha Singh.

Funding acquisition: James A. McNew, Michael Stern.

Supervision: James A. McNew, Michael Stern.

Writing – original draft: Kevin van der Graaf, Michael Stern.

Writing – review & editing: Kevin van der Graaf, James A. McNew, Michael Stern.

References

1. Thorpe HM, Smith MCM. In vitro site-specific integration of bacteriophage DNA catalyzed by a recombinase of the resolvase/invertase family. *Proc Natl Acad Sci.* 1998 May 12; 95(10):5505–10. <https://doi.org/10.1073/pnas.95.10.5505> PMID: 9576912
2. Groth AC. Construction of Transgenic Drosophila by Using the Site-Specific Integrase From Phage C31. *Genetics.* 2004 Apr 1; 166(4):1775–82. <https://doi.org/10.1534/genetics.166.4.1775> PMID: 15126397
3. Groth AC, Calos MP. Phage Integrase: Biology and Applications. *J Mol Biol.* 2004 Jan; 335(3):667–78. <https://doi.org/10.1016/j.jmb.2003.09.082> PMID: 14687564
4. Bateman JR, Lee AM, Wu C. Site-Specific Transformation of Drosophila via ϕ C31 Integrase-Mediated Cassette Exchange. *Genetics.* 2006 Jun 1; 173(2):769–77. <https://doi.org/10.1534/genetics.106.056945> PMID: 16547094
5. Venken KJT, He Y, Hoskins RA, Bellen HJ. [acman]: A BAC Transgenic Platform for Targeted Insertion of Large DNA Fragments in *D. melanogaster*. *Science* (80-). 2006 Dec 15; 314(5806):1747–51. <https://doi.org/10.1126/science.1134426> PMID: 17138868
6. Bischof J, Maeda RK, Hediger M, Karch F, Basler K. An optimized transgenesis system for Drosophila using germ-line-specific C31 integrases. *Proc Natl Acad Sci.* 2007 Feb 27; 104(9):3312–7. <https://doi.org/10.1073/pnas.0611511104> PMID: 17360644
7. Thorpe HM, Wilson SE, Smith MCM. Control of directionality in the site-specific recombination system of the Streptomyces phage phiC31. *Mol Microbiol.* 2000 Oct; 38(2):232–41. <https://doi.org/10.1046/j.1365-2958.2000.02142.x> PMID: 11069650
8. Zirin J, Hu Y, Liu L, Yang-Zhou D, Colbeth R, Yan D, et al. Large-Scale Transgenic Drosophila Resource Collections for Loss- and Gain-of-Function Studies. *Genetics.* 2020 Apr; 214(4):755–67. <https://doi.org/10.1534/genetics.119.302964> PMID: 32071193
9. Perkins LA, Holderbaum L, Tao R, Hu Y, Sopko R, McCall K, et al. The Transgenic RNAi Project at Harvard Medical School: Resources and Validation. *Genetics.* 2015 Nov 1; 201(3):843–52. <https://doi.org/10.1534/genetics.115.180208> PMID: 26320097
10. Markstein M, Pitsouli C, Villalta C, Celniker SE, Perrimon N. Exploiting position effects and the gypsy retrovirus insulator to engineer precisely expressed transgenes. *Nat Genet.* 2008 Apr 2; 40(4):476–83. <https://doi.org/10.1038/ng.101> PMID: 18311141
11. Larkin A, Marygold SJ, Antonazzo G, Attrill H, dos Santos G, Garapati P V, et al. FlyBase: updates to the Drosophila melanogaster knowledge base. *Nucleic Acids Res.* 2021 Jan 8; 49(D1):D899–907. <https://doi.org/10.1093/nar/gkaa1026> PMID: 33219682
12. De S, Cheng Y, Sun M, Gehred ND, Kassis JA. Structure and function of an ectopic Polycomb chromatin domain. *Sci Adv.* 2019 Jan 1; 5(1):eaau9739. <https://doi.org/10.1126/sciadv.aau9739> PMID: 30662949
13. Kim DI, Birendra KC, Roux KJ. Making the LINC: SUN and KASH protein interactions. *Biol Chem.* 2015 Apr; 396(4):295–310. <https://doi.org/10.1515/hsz-2014-0267> PMID: 25720065
14. Volk T. A new member of the spectrin superfamily may participate in the formation of embryonic muscle attachments in Drosophila. *Development.* 1992 Nov; 116(3):721–30. <https://doi.org/10.1242/dev.116.3.721> PMID: 1289062
15. McGee MD, Rillo R, Anderson AS, Starr DA. UNC-83 Is a KASH Protein Required for Nuclear Migration and Is Recruited to the Outer Nuclear Membrane by a Physical Interaction with the SUN Protein UNC-

84. Mol Biol Cell. 2006 Apr; 17(4):1790–801. <https://doi.org/10.1091/mbc.e05-09-0894> PMID: 16481402
16. Xie X, Fischer JA. On the roles of the *Drosophila* KASH domain proteins Msp-300 and Klarsicht. Fly (Austin). 2008; 2(2):74–81. <https://doi.org/10.4161/fly.6108> PMID: 18820482
17. Zheng Y, Buchwalter RA, Zheng C, Wight EM, Chen J V, Megraw TL. A perinuclear microtubule-organizing centre controls nuclear positioning and basement membrane secretion. Nat Cell Biol. 2020 Mar; 22(3):297–309. <https://doi.org/10.1038/s41556-020-0470-7> PMID: 32066907
18. Packard M, Jokhi V, Ding B, Ruiz-Cañada C, Ashley J, Budnik V. Nucleus to Synapse Nesprin1 Railroad Tracks Direct Synapse Maturation through RNA Localization. Neuron. 2015 May; 86(4):1015–28. <https://doi.org/10.1016/j.neuron.2015.04.006> PMID: 25959729
19. Volk T. Positioning nuclei within the cytoplasm of striated muscle fiber. Nucleus. 2013 Jan 28; 4(1):18–22. <https://doi.org/10.4161/nucl.23086> PMID: 23211643
20. Zhang J, Felder A, Liu Y, Guo LT, Lange S, Dalton ND, et al. Nesprin 1 is critical for nuclear positioning and anchorage. Hum Mol Genet. 2010 Jan; 19(2):329–41. <https://doi.org/10.1093/hmg/ddp499> PMID: 19864491
21. Morel V, Lepicard S, Rey AN, Parmentier M-L, Schaeffer L. *Drosophila* Nesprin-1 controls glutamate receptor density at neuromuscular junctions. Cell Mol Life Sci. 2014 Sep; 71(17):3363–79. <https://doi.org/10.1007/s00018-014-1566-7> PMID: 24492984
22. Yu J, Starr DA, Wu X, Parkhurst SM, Zhuang Y, Xu T, et al. The KASH domain protein MSP-300 plays an essential role in nuclear anchoring during *Drosophila* oogenesis. Dev Biol. 2006 Jan; 289(2):336–45. <https://doi.org/10.1016/j.ydbio.2005.10.027> PMID: 16337624
23. Rajgor D, Shanahan CM. Nesprins: from the nuclear envelope and beyond. Expert Rev Mol Med. 2013 Jul 5; 15:e5. <https://doi.org/10.1017/erm.2013.6> PMID: 23830188
24. Summerville JB, Faust JF, Fan E, Pendin D, Daga A, Formella J, et al. The effects of ER morphology on synaptic structure and function in *Drosophila melanogaster*. J Cell Sci. 2016 Apr 15; 129(8):1635–48. <https://doi.org/10.1242/jcs.184929> PMID: 26906425
25. Orso G, Pendin D, Liu S, Toso J, Moss TJ, Faust JE, et al. Homotypic fusion of ER membranes requires the dynamin-like GTPase atlastin. Nature. 2009 Aug; 460(7258):978–83. <https://doi.org/10.1038/nature08280> PMID: 19633650
26. Feng Y, Ueda A, Wu C-F. A modified minimal hemolymph-like solution, HL3.1, for physiological recordings at the neuromuscular junctions of normal and mutant *Drosophila* larvae. J Neurogenet. 2004; 18(2):377–402. <https://doi.org/10.1080/01677060490894522> PMID: 15763995
27. Livak KJ, Schmittgen TD. Analysis of Relative Gene Expression Data Using Real-Time Quantitative PCR and the 2- $\Delta\Delta$ CT Method. Methods. 2001 Dec; 25(4):402–8. <https://doi.org/10.1006/meth.2001.1262> PMID: 11846609
28. Lattao R, Bonaccorsi S, Guan X, Wasserman SA, Gatti M. Tubby-tagged balancers for the *Drosophila* X and second chromosomes. Fly (Austin). 2011; 5(4):369–70. <https://doi.org/10.4161/fly.5.4.17283> PMID: 21785267
29. Cyranowska C. Transcriptional Correlates of Homeostatic Plasticity and Neuronal Diversity at the Neuromuscular Junction. Ph.D. thesis. University of California; 2020.
30. Elhanany-Tamir H, Yu Y V., Shnyder M, Jain A, Welte M, Volk T. Organelle positioning in muscles requires cooperation between two KASH proteins and microtubules. J Cell Biol. 2012 Sep 3; 198(5):833–46. <https://doi.org/10.1083/jcb.201204102> PMID: 22927463
31. Nozawa K. The effects of the environmental conditions on Curly expressivity in *Drosophila melanogaster*. Japanese J Genet. 1956; 31(6):163–71.
32. Kolodkin AL, Pickup AT, Lin DM, Goodman CS, Banerjee U. Characterization of Star and its interactions with sevenless and EGF receptor during photoreceptor cell development in *Drosophila*. Development. 1994 Jul; 120(7):1731–45. <https://doi.org/10.1242/dev.120.7.1731> PMID: 7924981
33. Mirth C, Truman JW, Riddiford LM. The role of the prothoracic gland in determining critical weight for metamorphosis in *Drosophila melanogaster*. Curr Biol. 2005 Oct; 15(20):1796–807. <https://doi.org/10.1016/j.cub.2005.09.017> PMID: 16182527
34. van der Graaf K, Jindrich K, Mitchell R, White-Cooper H. Roles for RNA export factor, Nxt1, in ensuring muscle integrity and normal RNA expression in *Drosophila*. G3 Genes|Genomes|Genetics. 2021 Jan 1; 11(1):jkaa046. <https://doi.org/10.1093/g3journal/jkaa046> PMID: 33561245
35. Groen CM, Podratz JL, Pathoulas J, Staff N, Windebank AJ. Genetic Reduction of Mitochondria Complex I Subunits is Protective against Cisplatin-Induced Neurotoxicity in *Drosophila*. J Neurosci. 2022 Feb 2; 42(5):922 LP–937. <https://doi.org/10.1523/JNEUROSCI.1479-20.2021> PMID: 34893548

36. Duan Q, Estrella R, Carson A, Chen Y, Volkan PC. *Drosophila attP40* background alters glomerular organization of the olfactory receptor neuron terminals. bioRxiv. 2022 Jan 1;2022.06.16.496338. <https://doi.org/10.1101/2022.06.16.496338>